# Photoemission study of adsorbed Xe on GaAs(110), HgTe(110), and $Hg_{1-x}Cd_xTe(110)$ surfaces

G. Haugstad, A. Raisanen, X. Yu, L. Vanzetti, and A. Franciosi
*Department of Chemical Engineering and Materials Science, University of Minnesota, Minneapolis, Minnesota 55455*
(Received 30 August 1991; revised manuscript received 27 April 1992)

Synchrotron-radiation photoemission studies of Xe-atom physisorption at 35 K on cleaved GaAs(110) surfaces reveal the presence of a single first-layer adsorption site, followed at increasing coverage by the formation of a close-packed Xe second layer incommensurate with the substrate. Sizable binding-energy shifts of the Xe 4*d* and 5*p* levels from first to second adsorbed layer suggest non-negligible final-state screening of the photoemission-induced core hole by the GaAs substrate. Results for Xe atoms adsorbed on HgTe(110) and $Hg_{1-x}Cd_xTe(110)$ cleaved semiconductor surfaces show a similar initial adsorption site on all such surfaces, corresponding to an identical Xe 4*d* ionization energy of $66.3\pm0.1$ eV. We associate this common behavior to initial Xe adsorption at the high-coordination, fourfold-hollow site formed by anions on the (110) cleavage plane.

## INTRODUCTION

Photoemission from physisorbed Xe atoms has been recently employed to probe electrostatic potential variations across various metal and semiconductor substrates,[1–10] identify and titrate different adsorption sites,[2,3,6–9] and, in studies of thin films, gauge film morphology and metallicity.[4,5,8,10,11] For example, this technique revealed the existence of three inequivalent adsorption sites on the Si(111) $7\times7$ surface,[2,3] and identified island size, work function, and coalescence coverage during Yb-$Hg_{1-x}Cd_xTe$ interface formation.[5] We present here synchrotron-radiation photoemission studies of Xe atoms adsorbed on zinc-blende semiconductor surfaces cleaved *in situ*, with the goals of determining the corresponding adsorption sites, monitoring the development of a rare-gas solid film, and investigating the influence of the semiconductor surface on the ionization energy of the Xe electronic levels.

We examined in detail the coverage dependence of the Xe 4*d* and 5*p* photoemission line shapes for adsorption on GaAs(110) surfaces. We find, in contrast with the Si(111) $7\times7$ case,[2,3] a single adsorption site within the first Xe adsorbed layer. Xe 4*d* ionization energies for submonolayer amounts of Xe on cleaved HgTe(110), $Hg_{1-x}Cd_xTe(110)$, and *n*- and *p*-type GaAs(110) were found to be the same to within 0.1 eV, as expected for similar adsorption sites. We propose that for all of the compound semiconductor surfaces examined, Xe adsorption occurs initially at the anion-coordinated fourfold-hollow sites. The common Xe ionization energy at these sites is 0.6 eV greater than that observed for Xe adsorbed on metal substrates,[4] due to weaker final-state screening. Formation of a second Xe layer on GaAs(110) corresponds to a 0.5-eV increase in the apparent binding energy of the Xe 4*d* and 5*p* levels, due to a further reduction in the final-state screening, which involves primarily the valence orbitals of the outward-shifted anion first neighbors. The variation with Xe coverage of the Xe 5*p* line shape suggests the formation of a loosely packed first layer, commensurate with the substrate lattice, followed by the establishment of a close-packed, incommensurate second layer.

## EXPERIMENTAL DETAILS

Single-crystal posts $4\times4\times10$ mm$^3$ in size of HgTe, *p*-type $Hg_{0.78}Cd_{0.22}Te$, *n*-type GaAs, and *p*-type GaAs were cleaved in a photoelectron spectrometer at operating pressures in the low to mid $10^{-11}$-Torr range to expose mirrorlike (110) surfaces. Most GaAs(110) cleaved samples were in flat-band conditions at room temperature, and even in the worst cases the defect-induced band bending did not exceed 0.1–0.2 eV. Band bending was monitored *in situ* from the energy positions of the Ga 3*d* and As 3*d* core-level emission relative to the Fermi level. Cleaved HgTe(110) and $Hg_{0.78}Cd_{0.22}Te(110)$ surfaces were generally *n* type as a result of cleavage-induced, Hg-related point defects.[12,13] The samples were cooled to $35\pm5$ K by attaching the holder to the cold head of a helium closed-cycle refrigerator by means of a short Cu braid. The temperature was monitored by a Au-Fe/chromel thermocouple at the end of the braid. The sample temperature was calibrated by mounting a Si dipole on test samples in the same geometry. Xe exposures in the 1–24 L range (1 L$=10^{-6}$ Torr sec) were produced by backfilling the spectrometer with research-grade (purity 99.995%) Xe at pressures in the $10^{-8}$-Torr range.

Synchrotron-radiation photoemission measurements were performed using a commercial hemispherical energy analyzer operating in the angle-integrated mode. The photon source was the 800-MeV electron storage ring Aladdin at the Synchrotron Radiation Center of the University of Wisconsin-Madison. Photons were monochromatized by either a six-meter toroidal grating or a grasshopper Mark V grazing-incidence monochromator, with a measured overall experimental resolution (electrons+photons) varying from 0.2 to 0.4 eV for photon energies in the 40–130-eV range. Care was taken to select similar energy resolutions on different monochromators. Photoelectron energy-distribution curves (EDC's) were normalized to the photon flux monitored

 ©1992 The American Physical Society

using a Ni or W mesh. We used the Xe $4d$ and semiconductor core photoemission intensities to determine the Xe coverage via the photoelectron escape depth $\lambda$ in Xe. The procedure involved the determination of relative escape depths in the 20–70-eV kinetic-energy range through studies of multilayers of Xe on a variety of metal substrates.[14] From the observed plots of substrate and Xe core emission intensities as a function of Xe exposure, we obtained an escape depth increasing linearly as a function of logarithmic kinetic energy, in the kinetic-energy range examined. A linear extrapolation was therefore used to estimate the escape depth at higher kinetic energies.

Absolute values of the escape depths (in Å) at selected photon energies were determined by three methods, producing consistent results: (1) we decomposed[15] the Xe $4d$ high-resolution spectra of a thick ($\approx 50$ Å), homogeneous Xe film into bulk-related and surface-shifted contributions.[16] Comparison of surface- and bulk-derived emission intensities yielded the escape depth; (2) we used the published values of the attenuation of first-layer Xe features on metals due to adsorption of a second Xe layer (Ref. 16 at $h\nu = 90$ eV) to determine the photoelectron escape depth; (3) we compared the coverage dependence of the Xe $4d$ emission intensity for first- and second-layer Xe adsorption at $T = 12$ K on high work-function metals[17] to the results of Monte Carlo simulations, assuming unity sticking coefficient and no Xe surface diffusion. The escape depth $\lambda$ was used as an adjustable parameter, and the best fit condition determined $\lambda$.[17] These three methods yielded consistent photoelectron escape depths in Xe; $\lambda = 5.5 \pm 0.5$ and $8.5 \pm 1$ Å at kinetic energies of 23 and 105 eV, respectively.

Analysis of the Xe $4d$ and $5p$ photoemission line shapes was performed to determine the number of line-shape components, their energy position, and relative intensity. EDC's for the $4d$ levels were approximated by one or two spin-orbit-split doublets; least-squares fits of the composite line shape were obtained using a superposition of Voigt functions, one for each branch of a given doublet. The values of spin-orbit splitting and Lorentzian half-width at half maximum (HWHM) were fixed at values obtained previously,[4,5,19] while the position, intensity, Gaussian full width at half maximum (FWHM), and branching ratio were used as fitting parameters. For the Xe $5p$ line-shape analysis, individual $5p_{1/2}$, $5p_{3/2}$ $(m_j = \pm\frac{1}{2})$, and $5p_{3/2}$ $(m_j = \pm\frac{3}{2})$ components were also approximated by Voigt functions. Here, position, intensity, and Gaussian FWHM of each component, and a common Lorentzian HWHM for all components, were treated as fitting parameters. The secondary electron background was included in all fitting procedures as a third-order polynomial with coefficients determined together with the line-shape parameters through the fit.

## RESULTS AND DISCUSSION

In Fig. 1 we present representative EDC's for the Xe $4d$ emission as a function of Xe coverage for Xe condensed at $T = 35 \pm 5$ K onto $n$-type GaAs(110), with $h\nu = 90$ eV (solid circles). The binding-energy scale is referenced to the spectrometer Fermi level. Xe coverages $\Theta$ are shown to the right of each spectrum, increasing from 0.3 to 2.0 monolayers (ML) (bottom to top). We determined the coverage from the observed attenuation of the substrate core emission upon Xe adsorption. For example, the topmost spectrum in Fig. 1 was obtained after exposure to 16 L of xenon; the corresponding attenuation of the Ga $3d$ core emission was 65–70 %. For a photoelectron escape depth of $8.5 \pm 1.0$ Å, appropriate for a Ga $3d$ photoelectron kinetic energy of 105 eV ($h\nu = 130$ eV), this attenuation corresponds to a Xe thickness of about 7 Å, i.e., 2 ML. Such a coverage was also found to be the saturation coverage on the GaAs(110) surface at $35 \pm 5$ K, since further exposure to Xe resulted in no detectable increase in the Xe emission or decrease in the substrate emission, to within $\pm 2\%$. The implication is that at a substrate temperature of $35 \pm 5$ K only two monolayers of Xe on GaAs(110) are stable at $p \approx 10^{-11}$ Torr.[18]

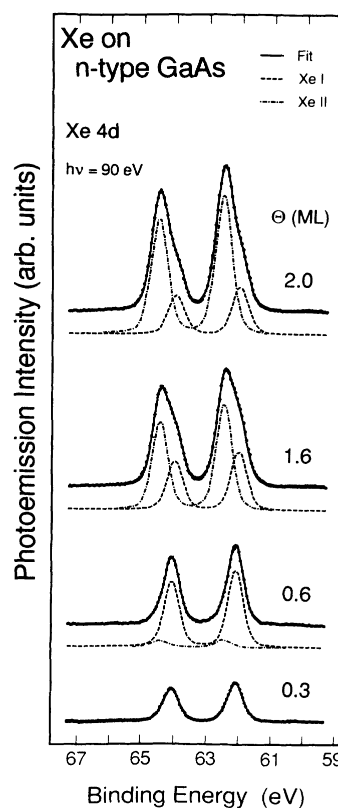


FIG. 1. EDC's at $h\nu = 90$ eV for the Xe $4d$ emission from Xe atoms physisorbed at $35 \pm 5$ K on cleaved $n$-type GaAs(110) (solid circles). Each spectrum was selected to represent a qualitatively different range of $4d$ line shapes as a function of increasing Xe coverage (bottom to top) in ML. Photoemission intensity is plotted in relative units and the binding-energy scale is referred to the spectrometer Fermi level. We also show superimposed to the data the result of a least-squares best fit in terms of a superposition of Lorentzian lines convoluted with a Gaussian broadening function (Voigt functions). The resulting individual Xe $4d$ doublets (dashed and dot-dashed line) are denoted Xe I and Xe II and correspond to Xe atoms in the first and second adsorbed layer, respectively.

The Xe 4*d* photoemission intensity in Fig. 1 is plotted in relative units. Each spectrum in Fig. 1 was selected to represent a qualitatively different range of 4*d* line shapes. The bottommost spectrum ($\Theta=0.3$ ML) is representative of the initial range of exposures at which a single, spin-split Xe 4*d* doublet is apparent. The second bottommost spectrum ($\Theta=0.6$ ML) is representative of the coverage range at which a second 4*d* doublet becomes visible to the left of the initial doublet. The third spectrum ($\Theta=1.6$ ML) is representative of the coverage range at which the second doublet becomes dominant. The topmost spectrum ($\Theta=2.0$ ML) is representative of the Xe saturation coverage. The results of best fits of the Xe 4*d* line shape in terms of a superposition of Voigt functions are shown in Fig. 1 (solid line) and contain either one (at 0.3 ML) or two 4*d* doublets (at higher coverages).[19] The individual doublets resulting from the fitting procedure are also shown, displaced downward for clarity. We will indicate with Xe 4*d* I the doublet with lower apparent binding energy (dashed line) and with Xe 4*d* II the doublet with higher apparent binding energy (dot-dashed line). We find that all Xe core features in Fig. 1 have the same Voigt linewidth at all Xe coverages. The Xe $4d_{5/2}$ binding energy relative to the Fermi level is $62.09\pm0.02$ eV at $\Theta=0.3$ and 0.6 ML, while at $\Theta=1.6$ and 2.0 LM it has shifted rigidly to $62.02\pm0.02$ eV. The Xe 4*d* II doublet (dot-dashed curve) has a $4d_{5/2}$ binding energy of $62.51\pm0.03$ eV.[20]

Since the Xe 4*d* II emission becomes dominant and the Xe 4*d* I emission intensity decreases as the Xe coverage approaches two monolayers, the simplest interpretation would associate the Xe 4*d* II features with Xe atoms within the second adsorbed layer. This interpretation is quantitatively consistent with the observed 4*d* I/4*d* II ratio for $\Theta=2$ ML. In the topmost EDC of Fig. 1 the ratio of the integrated emission intensities is $0.34\pm0.03$, and with a photoelectron escape depth of 5.5 Å, condensation of a Xe(111) monolayer (3.54 Å) would be expected to yield a first layer to second layer emission intensity ratio of $0.40\pm0.03$. We therefore identify the Xe 4*d* I and Xe 4*d* II features with first and second Xe layer emission, respectively. The 0.07-eV shift of the Xe 4*d* I component to lower binding energy upon the appearance of a large Xe 4*d* II component[21] mirrors what has been observed during studies of Xe condensation on single-crystal metal[16] or graphite substrates,[22] and associated with increased dielectric screening in a Xe bilayer relative to a single layer.

In photoemission studies of the Xe $5p_{1/2}$ emission from Xe adsorbed on Si(111) $7\times7$ surfaces,[2,3] three Xe emission features separated by up to 0.45 eV were observed at submonolayer coverages, and associated with inequivalent sites in the $7\times7$ unit cell, having different Xe adsorption energies. Highest-coordination sites would fill first,[2,3] as has been seen for Xe on metal surface.[7] In Fig. 1 we observe only Xe 4*d* emission features associated with first- and second-layer Xe atoms, indicating that most of the first-layer adsorption sites on GaAs(110) are equivalent within experimental uncertainty.

We propose that Xe atoms within the first layer adsorb preferentially at the high-coordination, fourfold-hollow sites,[23] where a Xe atom would be coordinated with four outwardly displaced As atoms,[23] which form a rectangle $4.00\times5.65$ Å in dimension. These are known to be the preferred chemisorption sites for metal atoms on GaAs(110) when the adatom-substrate interaction is relatively weak and surface mobility is high.[24,25] These sites, which exist prior to Xe adsorption, are also present after Xe adsorption, since upon Xe condensation the Ga 3*d* and As 3*d* core line shapes, comprised of two 3*d* doublets associated with emission from atoms in the bulk and surface (buckled) regions, remain unchanged.[17] We rule out that any of the Xe features observed in Fig. 1 might be related to Xe atoms adsorbed at cleavage steps, since a defect density large enough to yield detectable Xe features in Fig. 1 (1–5%) would pin the Fermi level at midgap,[26] and this was not observed at 300 K.

An observation which is fully consistent with our identification is that the onset of second-layer Xe emission is seen in Fig. 1 at Xe coverages $\Theta\approx0.6$ ML. The number of fourfold-hollow sites is $4.42\times10^{14}$ cm$^{-2}$, or 72% of the surface atomic density in close-packed Xe(111). Since the coverages in Fig. 1 were calculated in terms of the Xe(111) planar density (see preceding section), we expect that most of the fourfold-hollow sites are occupied for $\Theta\approx0.7$ ML.[27] The large size of the Xe atom (4.33 Å diameter) should inhibit accomodation of additional first-layer adatoms at other sites, and the onset of second-layer emission should be observed exactly in this coverage range.

Another quantity that should, in principle, reflect the number of first-layer sites relative to second-layer sites would be the Xe 4*d* I/4*d* II ratio at the saturation coverage of 2 ML in Fig. 1. The experimental value of $0.34\pm0.03$, as explained earlier, is to be compared to the escape-depth-derived ratio of $0.40\pm0.03$, expected if the first and second layers have the same planar atomic density. If the first layer is comprised only of the fourfold-hollow sites, then the planar density of the first layer would be only 72% that of a close-packed second layer,[27] and the expected ratio would be $0.29\pm0.03$. Unfortunately, both predicted values are consistent with the experimental ratio within the quoted uncertainties, which derive from the uncertainty on the measured integrated intensity ratios ($\pm10\%$) and the measured escape depth ($\pm10\%$). The overall uncertainty in the Xe coverage is $\pm0.3$ ML at a nominal coverage of 1.0 ML, and $\pm0.4$ ML at 2.0 ML. The magnitude of the latter uncertainty makes it impossible to distinguish with certainty between a 2.0-ML or 1.7-ML equivalent close-packed coverage using solely the relevant intensity data.

The energy separation between first- and second-layer Xe 4*d* doublets implies differences in the initial- or final-state interaction with the substrate electrons. We believe that final-state effects are the main factor behind the observed shift. Initial-state effects, which include chemical interactions, and possible perturbations of the vacuum-level alignment,[28] are unlikely on the basis of several considerations. Chemical interactions are, in general, negligible for a physisorbed inert gas.[29] Perturbations of the vacuum-level alignment would likely be associated with the overlap of Xe valence orbitals and substrate regions

of varying potential,[28] or physisorption-induced polarization of first-layer Xe atoms.[30] The first effect would have as a consequence that the reference for Xe energy levels would no longer be the local vacuum level, but rather a value between the vacuum level and the mean electrostatic potential inside the substrate.[28] This would shift the first-layer (Xe I) energy levels to higher binding energy relative to the vacuum-level referenced second-layer (Xe II) emission. We rule out this effect here by noting that the observed Xe $4d$ I binding energy is, in fact, lower than that of Xe $4d$ II. The other mechanism of perturbation in vacuum-level alignment, namely a strong physisorption-induced polarization of first-layer Xe atoms, would yield a dipole layer that would reduce the net work function, so second-layer Xe energy levels would be shifted (relative to first layer) to higher binding energy.[30] We rule out also this type of initial-state effect by noting that Xe-semiconductor interactions are known to be weaker than Xe-metal interactions[1,3] and, in the latter case, Xe polarization-induced shifts are typically only $\approx 0.1$ eV.[30]

Possible final-state contributions to layer-dependent energy shifts include long-range screening by substrate conduction electrons[4,16,30] and/or short-range screening by bound valence electrons.[1] Only the latter may be significant here, since the number of conduction electrons in the doped samples used ($10^{18}$ cm$^{-3}$, at least four orders of magnitude less than in metals) is not large enough to provide the metallic image-charge screening commonly observed on metals.[4,16,30] We propose that screening of the final-state $4d$ hole on the first-layer Xe atoms occupying the fourfold-hollow sites on GaAs(110) predominantly involves the valence electrons of the four outward-shifted As atoms.[31] Such a screening would be negligible for second-layer atoms and explains the observed Xe $4d$ I-Xe $4d$ II shift.

In their study of Xe adsorbed on Si(111) 7×7 surfaces, Demuth and Schell-Sorokin[2] observed a 0.5-eV increase in $5p_{1/2}$ binding energy in comparing the dominant first-layer component and a "condensed" Xe component seen at $\Theta = 2.5$ ML. A mechanism was not proposed by these authors, but final-state screening by (localized) substrate valence electrons seems to us the only plausible explanation. This effect thus would appear to be significant for both compound and elemental semiconductors. We expect it to be weaker on many metal surfaces investigated,[4,16,30] since the large size of Xe atoms, relative to the metal substrate corrugation, restricts the Xe orbitals to a region beyond the spatial extent of substrate valence orbitals.[29]

Results for Xe condensation on a number of cleaved compound semiconductor surfaces are shown in Fig. 2. Xe $4d$ EDC's for 0.3–0.5 ML of Xe adsorbed at $T = 35 \pm 5$ K on HgTe(110), $p$-type $Hg_{1-x}Cd_xTe$(110), and $n$- and $p$-type GaAs(110) (top to bottom) are presented, at a photon energy of 130 eV (solid circles). The EDC's in Fig. 2 are plotted as a function of ionization energy, i.e., the zero of the energy scale was referenced to the vacuum level. This was done by adding the most reliable published values of photoemission threshold energies (HgTe: 5.9 eV, Ref. 32; $Hg_{0.78}Cd_{0.22}Te$: 6.0 eV, Ref. 33; GaAs: 5.56 eV, Ref. 34) to binding energies measured relative to the substrate valence-band maximum.[35] The latter was estimated from a least-squares linear extrapolation of the leading valence-band edge. A single Xe $4d$ doublet is observed at this Xe coverage on all semiconductors, with an average $4d_{5/2}$ peak position of $66.3 \pm 0.1$ eV (solid vertical line in Fig. 2) relative to the vacuum level in the series. The result of a fit in terms of Voigt functions is also shown in Fig. 2 (solid line) superimposed with the data.[36] The compelling similarity in $4d$ position and line shape suggests that the same type of adsorption site is present for Xe on all of these semiconductors, and that only this site is populated at coverages of 0.3–0.5 ML on HgTe(110) and $Hg_{0.78}Cd_{0.22}Te$(110), as found for GaAs(110).[37]

We propose that on the (110) surface of cleaved zinc-blende semiconductors the fourfold-hollow site formed by anions is, in general, the preferred site for adsorption. Whether at higher coverages other sites are populated on HgTe and $Hg_{0.78}Cd_{0.22}Te$ remains to be seen. The density of the fourfold-hollow sites on these surfaces is only

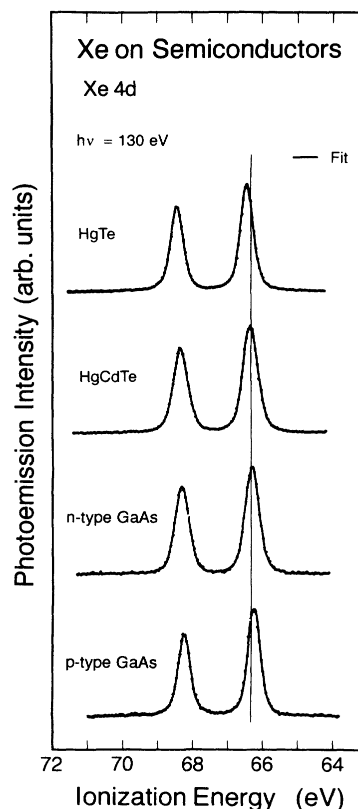


FIG. 2. EDC's at $h\nu = 130$ eV for the Xe $4d$ emission from submonolayer coverages of Xe (0.3–0.5 ML) on various semiconductor (110) cleavage surfaces at $35 \pm 5$ K (solid circles). The binding-energy scale was referenced to the vacuum level by adding published values of the substrate photoemission threshold energies to binding energies measured relative to the substrate valence-band edge. We also show superimposed the result of a least-squares best fit of the data in terms of a superposition of Voigt functions.

56% of the atomic density of Xe (111), but the accomodation of additional first-layer Xe atoms would probably require a film reconstruction. The resulting value of the Xe $4d_{5/2}$ ionization energy (66.3±0.1 eV) on the surfaces of the semiconductors in Fig. 2, is 0.6 eV higher than that (65.7±0.1 eV, Ref. 4) observed for Xe atoms adsorbed on a variety of polycrystalline metal surfaces. The implication is that image charge screening by conduction electrons in a metal is significantly more effective than the short-range screening by semiconductor anion surface orbitals.

In order to compare Xe-level ionization energies for the semiconductors considered here directly with those for Xe condensed on ZnO (Ref. 1) and Si(111) 7×7 (Refs. 2 and 3), we need to examine the Xe 5*p* levels, the only Xe levels accessible to the authors of Refs. 1–3. In Fig. 3 we present incremental EDC's for the Xe 5*p* emission for Xe on GaAs(110) in relative units, with the incremental Xe coverage shown to the right of each, using $h\nu = 80$ eV. Binding energies are measured relative to the spectrometer Fermi level. To obtain the bottommost spectrum in Fig. 3 we subtracted the clean GaAs valence-band emission from data taken at a Xe coverage of 0.3 ML. The second, third, and fourth difference curves from the bottom in Fig. 3 were obtained subtracting the normalized raw data at coverages of 0.3, 0.6, and 1.6 ML from those at coverages of 0.6, 1.6, and 2.0 ML, respectively. The 5*p* doublets in Fig. 3 clearly display a broadened $j=\frac{3}{2}$ branch relative to the $j=\frac{1}{2}$ branch. For the bottommost two spectra, mostly reflecting the Xe first-layer emission, the broadening is relatively slight, while for the two topmost spectra, mostly reflecting the Xe second-layer emission, it is quite dramatic (note the FWHM markers, horizontal arrows, in Fig. 3), and a shoulder appears on the low-binding-energy side of the $j=\frac{3}{2}$ branch (see vertical bars).

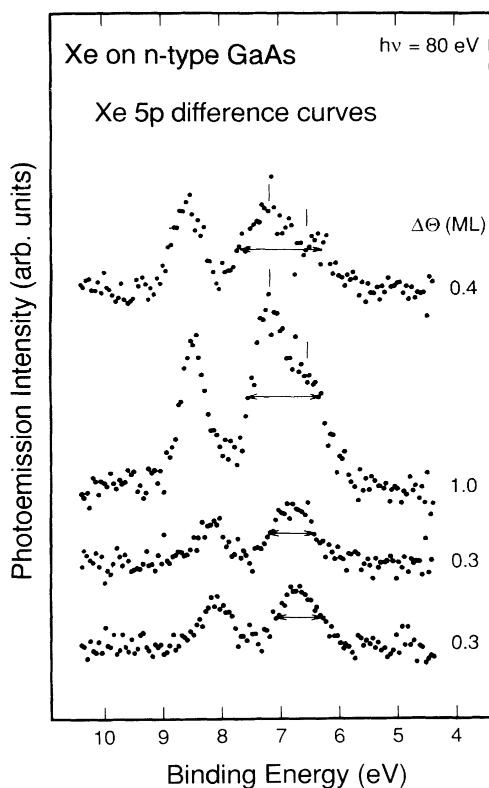


FIG. 3. EDC's at $h\nu = 80$ eV for incremental Xe 5*p* emission from atoms physisorbed at $T = 35 \pm 5$ K on cleaved *n*-type GaAs(110) (solid circles). The photoemission intensity is plotted in relative units. The bottommost spectrum was obtained by subtracting the valence emission from data taken with a Xe coverage of 0.3 ML. The second, third, and fourth spectra from the bottom were obtained by subtracting the normalized valence emission at 0.3, 0.6, and 1.6 ML from that at 0.6, 1.6, and 2.0 ML, respectively. The incremental coverages are indicated to the right of the corresponding spectra. The bottom two spectra correspond to emission from the first layer of Xe atoms, while the top two result predominantly from second-layer emission, and display a splitting of the $j=\frac{3}{2}$ branch characteristic of close-packed Xe atoms. The splitting is designated approximately by tick marks, and the $j=\frac{3}{2}$ branch FWHM by horizontal bars.

The first-layer Xe $5p_{1/2}$ emission appears (bottommost difference curves in Fig. 3) at a binding energy of 8.1 eV relative to the Fermi level, corresponding to an ionization energy of 12.1 eV.[38] For the second-layer emission (topmost difference curves in Fig. 3) the corresponding ionization energy is 12.5 eV. The latter is in good agreement with the results of Gutmann *et al.*,[1] who observed a $5p_{1/2}$ line shape centered at an ionization energy of 12.4±0.1 eV at Xe coverages ≥1 ML on three different faces of ZnO. The former is also in qualitative agreement with observations on ZnO since, at low coverage on the anion-terminated surface, the $5p_{1/2}$ ionization energy was reduced by 0.5 eV relative to the multilayer value.[1] The influence of ZnO(0001) surface oxygen atoms and GaAs(110) outward-shifted arsenic atoms on the Xe atoms adsorbed at "deep" sites appears, therefore, similar.[39]

In the two reports available on Si(111) 7×7 (Refs. 2 and 3), Xe $5p_{1/2}$ binding energies are given relative to the Fermi level, for *p*-type[2] and *n*-type[3] substrates. The 5*p* positions for the two minority Xe first-layer sites relative to the dominant first-layer sites (which account for 65–76 % of the total 5*p* intensity) are 0.10 and 0.45 eV to lower binding energy in the report by Demuth and Schell-Sorokin,[2] while Markert *et al.*[3] report binding energies 0.17 and 0.30 eV lower than that of the dominant feature. The disparity is probably due to uncertainties in extracting the precise location of these weak features. We therefore concern ourselves only with the 5*p* position for Xe atoms occupying the majority first-layer sites. To convert binding energies to ionization energies we add the Si photothreshold energy (5.10 eV, Ref. 40) to the Xe $5p_{1/2}$ binding energy referenced to the valence-band maximum. The latter quantity is obtainable only for the data of Demuth and Schell-Sorokin,[2] where valence-band photoemission spectra show explicitly the position of the Fermi level at the valence-band maximum, indicating flat-band conditions.[41] This method yields a Xe $5p_{1/2}$ ionization energy of 12.45 eV for the dominant first-layer 5*p* component, and implies a ≈12.95-eV 5*p* ionization ener-

gy for the condensed component, seen at $\Theta \approx 2.5$ ML. Such values are some 0.5 eV larger than those observed on GaAs(110) and ZnO, possibly implying a qualitatively different adsorption configuration for Xe on elemental and compound semiconductor cleavage surfaces. Further comparative photoemission studies of Xe physisorption on polar and nonpolar surfaces of elemental and compound semiconductors, as well as reconstructed versus unreconstructed surfaces, are necessary to shed light on the origins of these differences.

The Xe $5p$ emission can also be used to gain information on the coverage-dependent formation of the Xe band structure. The Xe $5p$-related bands have been studied for Xe atoms physisorbed on single-crystal metal (see Mariani, Horn, and Bradshaw[39] and Refs. 30 and 42) and graphite substrates.[43] As nearest-neighbor Xe-atom distances decrease, the Xe $5p_{3/2}$ branch broadens. A complete close-packed Xe(111) layer displays a two-dimensional band structure containing three bands, corresponding to the $5p_{1/2}$, $5p_{3/2}$ ($m_j = \pm\frac{1}{2}$), and $5p_{3/2}$ ($m_j = \pm\frac{3}{2}$) branches.[30,39,42,43] The qualitative change in Xe $5p_{3/2}$ level between first- and second-layer emission in Fig. 3 reflects the splitting of the $j = \frac{3}{2}$ branch, and suggests the formation of a close-packed second layer. The approximate positions of the $m_j = \pm\frac{1}{2}$ and $\pm\frac{3}{2}$ components are designated by vertical bars for the two spectra, at binding energies of 6.6 and 7.2 eV, respectively.

A decomposition of the $5p$ line shape in terms of the different $m_j$-related branches is included in Fig. 4. On the left-hand side we show EDC's at $h\nu = 80$ eV in relative units (solid circles) after subtraction of the comparatively weak GaAs(110) valence-band emission, with binding energies referenced to the Fermi level. In Figs. 4(a) and 4(b) we show the results of a best fit of the data (solid line) in terms of individual $j = \frac{1}{2}$ and $\frac{3}{2}$ Voigt functions (dashed lines) at Xe coverages where only the Xe $5p$ I (first layer) emission is observed. For the higher Xe-coverage spectra in Figs. 4(c) and 4(d), we subtracted the Xe $5p$ I contribution using the computer-generated line shape [Fig. 4(b), dashed line], normalized to the corresponding Xe $4d$ I intensity in Fig. 1. The remaining Xe $5p$ II (second-layer) contribution is shown on the right-hand side of Fig. 2. The $5p$ II line shape clearly contains more than one component in the $j = \frac{3}{2}$ branch. A superposition of three Voigt functions (dot-dashed lines) yields a very good fit (solid line) of the experimental data (solid circles).[44] The separation of the $5p_{1/2}$ and $5p_{3/2}$ ($m_j = \pm\frac{1}{2}$) components is $1.31 \pm 0.05$ eV, and the splitting between the two $j = \frac{3}{2}$ branches ($m_j = \pm\frac{1}{2}$ and $\pm\frac{3}{2}$) is about 0.65–0.7 eV. Both values are consistent with those expected for a close-packed Xe layer. Angle-resolved photoemission experiments by Mariani, Horn, and Bradshaw[39] and Mandel, Domke, and Kaindl[43] yielded a $5p_{1/2}$ and $5p_{3/2}$ ($m_j = \pm\frac{1}{2}$) separation of 1.25–1.35 eV, and a splitting between the two $j = \frac{3}{2}$ branches ($m_j = \pm\frac{1}{2}$ and $\pm\frac{3}{2}$) of 0.55–0.7 eV.[39]

The evolution of the $5p$ line shape in Fig. 4 strongly indicates that the second-layer emission (Xe II in Fig. 4), unlike the first-layer emission, reflects close packing of Xe atoms, so that the second-layer Xe atoms are necessarily out of registry with substrate adsorption sites. We mention that Hong and Birgeneau,[45] during studies of Xe condensation on graphite ($T < 55$ K), have also observed a commensurate first layer, followed by incommensurate second and third layers. How general this type of growth mode is for Xe on semiconductors remains to be ascer-

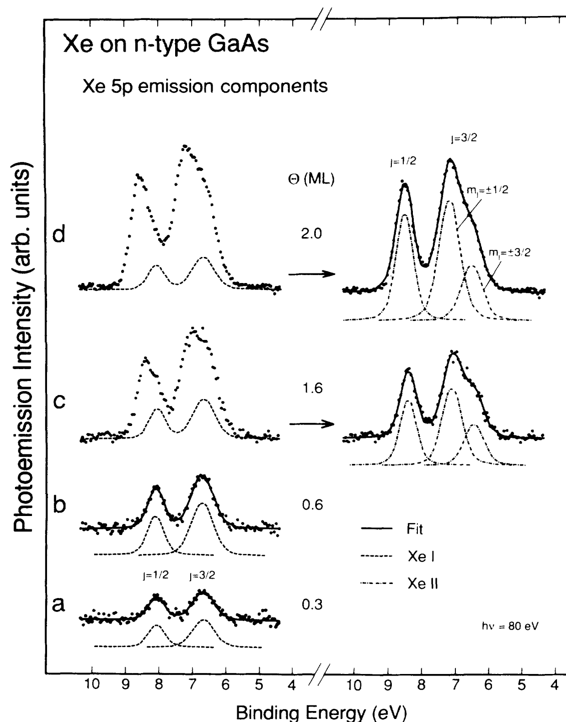


FIG. 4. EDC's at $h\nu = 80$ eV for the Xe $5p$ emission from atoms adsorbed at $T = 35 \pm 5$ K on cleaved $n$-type GaAs(110) (solid circles). The photoemission intensity is plotted in relative units, and binding energies are referenced to the spectrometer Fermi level. Data on the left are shown following the subtraction of the GaAs(110) valence-band emission. Xe coverages in monolayers (ML) are shown in the center of the figure. The data (solid circles) are shown superimposed with the result of a least-squares fit in terms of Voigt functions. The fit line shape at $\Theta = 0.6$ ML has been reduced in intensity (following the Xe $4d$ fit) and subtracted from the data at $\Theta = 1.6$ and 2.0 ML, producing the data at the upper right (solid circles). Superimposed on these spectra are similar fits containing three singlets (dot-dashed lines), corresponding to emission from second-layer atoms. (a) Xe $5p$ emission at $\Theta = 0.3$ ML reflects the $j = \frac{1}{2}$ and $\frac{3}{2}$ branches (dashed line) of the Xe first-layer emission. (b) Xe $5p$ emission at $\Theta = 0.6$ ML is also well reproduced by two first-layer Voigt functions (dashed line). (c) Xe $5p$ emission at $\Theta = 1.6$ ML (left, solid circles) after subtraction of the first-layer contribution (left, dashed line) yields the second-layer contribution (right, solid circles) which is well reproduced by three Voigt functions (right, dot-dashed line), corresponding to the $j = \frac{1}{2}$ and $\frac{3}{2}$ ($m_j = \pm\frac{1}{2}$ and $\pm\frac{3}{2}$) branches of close-packed Xe. (d) Xe $5p$ emission at $\Theta = 2$ ML (left, solid circles), after subtraction of the first-layer emission (dashed line), also shows (right) the three branches characteristic of close-packed Xe.

tained, since very few experiments sensitive to Xe-Xe distances have been conducted so far on these intriguing systems.

## CONCLUSIONS

Photoemission studies of Xe atoms physisorbed on cleaved GaAs(110) $1\times1$ surfaces reveal a single first-layer adsorption site, in contrast to results for Si(111) $7\times7$, where three sites have been reported. Additional results for Xe on HgTe(110) and $Hg_{1-x}Cd_xTe(110)$ surfaces are compellingly similar to those for Xe on GaAs(110), at least in the low-Xe coverage regime examined, and suggest the presence of a common type of adsorption sites on this class of surfaces. We propose that Xe adsorption occurs at the fourfold-hollow sites on all such surfaces. The apparent 4*d* ionization energy for Xe atoms adsorbed on these sites is about 0.6 eV larger than that found in studies of Xe on metals, as a result of the reduced final-state screening of the Xe 4*d* core hole by the semiconductor states. We attribute to the anion-derived semiconductor valence orbitals a primary role in screening the Xe core hole. Condensation of a second Xe layer on GaAs(110) produces Xe 5*p* spectral features characteristic of the formation of a close-packed second Xe layer, necessarily incommensurate with the substrate lattice. Correspondingly, the ionization energies of 5*p* and 4*d* levels in second-layer Xe atoms become 0.4–0.5 eV greater than those observed for the first-layer atoms, due to the reduction is screening from the relatively localized anion-derived orbitals. Earlier Xe physisorption results on the anion-terminated ZnO surfaces yielded Xe 5*p* ionization energies in good agreement with those found here. In contrast, reported 5*p* ionization energies on Si(111) $7\times7$ are about 0.5 eV larger. Studies in progress will clarify how generally different Xe adsorption is on compound versus elemental semiconductors by examining polar versus nonpolar surfaces, as well as reconstructed versus unreconstructed surfaces.

## ACKNOWLEDGMENTS

This work was supported by the Office of Naval Research under Grant No. N00014-89-J-1407 and by the Center for Interfacial Engineering of the University of Minnesota. We are in debt to J. E. Demuth, M. H. Hecht, K. Horn, K. Jacobi, M. Onellion, and K. Wandelt for useful discussions, and for providing us with their results prior to publication. The synchrotron-radiation photoemission measurements presented here were performed at the Synchrotron Radiation Center of the University of Wisconsin-Madison, supported by NSF. We gratefully acknowledge the cheerful assistance of its staff.

---

[1]A. Gutmann, G. Zwicker, D. Schmeisser, and K. Jacobi, Surf. Sci. **137**, 211 (1984).

[2]J. E. Demuth and A. J. Schell-Sorokin, J. Vac. Sci. Technol. A **2**, 808 (1984).

[3]K. Markert, P. Pervan, W. Heichler, and K. Wandelt, Surf. Sci. **211/212**, 611 (1989).

[4]G. Haugstad, A. Raisanen, L. Sorba, L. Vanzetti, X. Yu, and A. Franciosi, J. Vac. Sci. Technol. B **9**, 2415 (1991).

[5]A. Raisanen, G. Haugstad, X. Yu, G. Ceccone, and A. Franciosi, J. Vac. Sci. Technol. A **8**, 3265 (1990); A. Franciosi, A. Raisanen, G. Haugstad, G. Ceccone, and X. Yu, Phys. Rev. B **41**, 7914 (1990).

[6]H. H. Rottermund and K. Jacobi, Surf. Sci. **126**, 32 (1983).

[7]R. Miranda, S. Daiser, K. Wandelt, and G. Ertl, Surf. Sci. **131**, 61 (1983).

[8]M. Alnot, V. Gorodetskii, A. Cassuto, and J. J. Ehrhardt, Surf. Sci. **162**, 886 (1985).

[9]R. Ducros, J. J. Ehrhardt, J. Fusy, and B. Mutaftschiev, Phys. Rev. B **38**, 10 035 (1988).

[10]D. R. Mullins, J. M. White, and H. S. Luftman, Surf. Sci. **167**, 39 (1986).

[11]M. Onellion and J. L. Erskine, Surf. Sci. **177**, L983 (1986).

[12]H. M. Nitz, O. Ganschow, U. Kaiser, L. Wiedmann, and A. Benninghoven, Surf. Sci. **104**, 365 (1981).

[13]P. M. Raccah, U. Lee, J. A. Silberman, W. E. Spicer, and J. A. Wilson, Appl. Phys. Lett. **42**, 374 (1983).

[14]G. Haugstad, C. Caprile, A. Franciosi, D. M. Wieliczka, and C. G. Olson, J. Appl. Phys. **70**, 7333 (1991).

[15]This was achieved through a simple analysis method described, for example, by D. E. Eastman, T.-C. Chiang, P. Heimann, and F. J. Himpsel, Phys. Rev. Lett. **45**, 656 (1980).

[16]T.-C. Chiang, G. Kaindl, and T. Mandel, Phys. Rev. B **33**, 695 (1986).

[17]G. Haugstad, Ph.D. thesis, University of Minnesota, 1992.

[18]It is expected that Xe dosing until a stable saturation coverage is reached will produce an integral number of layers, since the addition of each higher-order layer typically involves a first-order phase transition (see, for example, Ref. 7).

[19]Typical values of the 4*d* doublet line-shape parameters were spin-orbit splitting 1.98 eV, branching ratio 0.8, Lorentzian HWHM 0.09 eV, and Gaussian FWHM 0.5 eV. The value for the spin-orbit splitting is in agreement with that determined in high-resolution gas-phase studies by B. W. Yates, K. H. Tan, L. L. Coastsworth, and G. M. Bancroft, Phys. Rev. A **31**, 1529 (1985), and the values for branching ratio and Lorentzian FWHM agree with published values for the condensed state (thick film, $h\nu=90$ eV, Ref. 16).

[20]The uncertainties represent the total scatter (among all available spectra) of the fit-determined energy position of each component.

[21]This small shift was reproducibly observed on the six different cleaves examined.

[22]T. Mandel, M. Domke, G. Kaindl, C. Laubschat, M. Prietsch, U. Middelmann, and K. Horn, Surf. Sci. **162**, 453 (1985).

[23]R. M. Feenstra, J. A. Stroscio, J. Tersoff, and A. P. Fein, Phys. Rev. Lett. **58**, 1192 (1987).

[24]P. N. First, R. A. Dragoset, J. A. Stroscio, R. J. Celotta, and R. M. Feenstra, J. Vac. Sci. Technol. A **7**, 2868 (1989).

[25]B. M. Trafas, D. M. Hill, R. L. Siefert, and J. H. Weaver, Phys. Rev. B **42**, 3231 (1990).

[26]L. J. Brillson, Surf. Sci. Rep. **2**, 123 (1982).

[27]Evidence for a close-packed second Xe layer will be presented

later in this work. Close-packed Xe layers are known to form on metal and graphite substrates (see, for example, Refs. 30, 39, 42, 43, and 45); in Ref. 45 this was reportedly the case only for second- and higher-order layers.

[28]K. Wandelt and J. E. Hulse, J. Chem. Phys. **80**, 1340 (1984).

[29]N. D. Lang and A. R. Williams, Phys. Rev. B **25**, 2940 (1982).

[30]K. Jacobi, Phys. Rev. B **38**, 5869 (1988).

[31]Gutmann *et al.* proposed (Ref. 1) an analogous mechanism to explain a coverage-dependent energy shift of the Xe 5*p* emission observed during Xe adsorption on ZnO oxygen-terminated polar surfaces. The first adsorbed Xe atoms, coordinated with oxygen atoms, exhibited a 0.5-eV shift to lower binding energy of the 5*p* levels relative to the Xe atoms at monolayer coverage, which formed a close-packed layer.

[32]N. J. Shevchick, J. Tejeda, M. Cardona, and D. W. Langer, Phys. Status Solidi **59**, 87 (1973).

[33]For $Hg_{0.78}Cd_{0.22}Te$ we estimated a photoemission threshold energy of 6.0 eV by performing a linear interpolation between the values for HgTe (5.9 eV) and CdTe (6.2 eV) published in Ref. 32.

[34]J. Van Laar, A. Huijser, and T. L. van Rooy, J. Vac. Sci. Technol. **14**, 894 (1977).

[35]*In situ* measurements of sample work functions from the widths of the photoemission spectra were not performed, since the necessary electrostatic biasing of the sample was incompatible with the mechanical coupling used to control sample temperatures.

[36]The experiments were conducted using the same monochromator. Variations in FWHM for the four spectra are $<0.1$ eV.

[37]By contrast, our preliminary Xe 4*d* results for adsorption on cleaved Ge(111) $2\times1$ (not shown) reveal two adsorption sites at submonolayer coverages, titrated in a coverage-independent 3:1 ratio.

[38]For *n*-type GaAs the ionization energy is obtained to a good approximation ($\pm0.05$ eV) by adding the photoemission threshold energy (5.56 eV, Ref. 34) to the Fermi-level-referenced binding energy (8.1 eV), and subtracting the band-gap energy at $T=0$ K (1.52 eV).

[39]A 0.5-eV change in the Xe 5*p* energy in going from $\Theta=0.5$ to 1.0 ML on ZnO reflects a transition in film character (Ref. 1), possibly from a commensurate to incommensurate phase. See, for example, C. Mariani, K. Horn, and A. M. Bradshaw, Phys. Rev. B **25**, 7798 (1982); M. Jaubert, A. Glachant, M. Bienfait, and G. Boato, Phys. Rev. Lett. **46**, 1679 (1981); H. Hong, C. J. Peters, A. Mak, R. J. Birgeneau, P. M. Horn, and H. Suematsu, Phys. Rev. B **36**, 7311 (1987).

[40]G. W. Gobeli and F. G. Allen, Phys. Rev. **137**, A245 (1965).

[41]For the data of Markert *et al.* (Ref. 3) we do not know the exact position of the Fermi level relative to the valence-band maximum, and hence whether or not flat-band conditions exist.

[42]A. Cassuto, J. J. Ehrhardt, J. Cousty, and R. Riwan, Surf. Sci. **194**, 579 (1988).

[43]T. Mandel, M. Domke, and G. Kaindl, Surf. Sci. **197**, 81 (1988).

[44]For both $\Theta=1.6$ and 2.0 ML the $j=\frac{3}{2}$ singlets were somewhat broader than the $j=\frac{1}{2}$ singlet, by about 0.1 and 0.15 eV, respectively. This is qualitatively consistent with the relative Xe 5*p* band dispersion measured for several substrates. See Mariani, Horn, and Bradshaw (Ref. 39) and Refs. 42 and 43.

[45]H. Hong and R. J. Birgeneau, Z. Phys. B **77**, 413 (1989).